Journal of Molecular Catalysis A: Chemical 350 (2011) 49–55

Contents lists available at SciVerse ScienceDirect

Journal of Molecular Catalysis A: Chemical

journal homepage: www.elsevier.com/locate/molcata

Photocatalytic transformation of chlorophenols under homogeneous and heterogeneous conditions using palladium octadodecylthio phthalocyanine

Taofeek B. Ogunbayo, Tebello Nyokong*

Department of Chemistry, Rhodes University, Grahamstown 6140, South Africa

ARTICLE INFO

Article history:
Received 18 February 2011
Received in revised form 7 September 2011
Accepted 10 September 2011
Available online 16 September 2011

Keywords:
Chlorophenols
Photosensitizers
Singlet oxygen quantum yield
Palladium phthalocyanine

ABSTRACT

Homogeneous and heterogeneous photosensitized transformations of 4-chlorophenol (4-CP) and pentachlorophenol (PCP) using palladium octadodecylthiophthalocyanine (PdODPc) were investigated. Under heterogeneous conditions, the photosensitizer was supported on functionalized single walled carbon nanotubes (SWCNTs). Homogeneous photosensitization proved to be more effective than the heterogeneous reaction in terms of percentage of transformation achieved. The kinetics of heterogeneous catalysis proved that ads-PdODPc–SWCNT–COOH (where SWCNT has been functionalized with COOH groups) was reusable for 4-CP while its activity degenerated when reused for PCP. Singlet oxygen was confirmed as playing an active role in the reactions.

1. Introduction

The environmental pollution by chlorophenols has been well documented [1–3]. There has been considerable investigation of degradation of phenols using oxidants in the presence of catalysts such as metallophthalocyanines (MPcs). Using oxidants has proved successful with chlorophenols (and related molecules) degraded to less harmful products such as CO_2 [4–10]. However, processes involving no oxidants are still preferred.

Due to their high absorption in the visible region and singlet oxygen generating ability, MPc complexes have been used as homogeneous and heterogeneous photocatalysts [11–15]. In spite of the advantage of ease of catalyst regeneration associated with heterogeneous catalysis, homogeneous catalysis holds the potential for kinetic studies of the photodegradation reactions and easier understanding of the mechanisms involved in the reaction.

Open-shell metallophthalocyanines produce large triplet state quantum yields and efficiently generate singlet oxygen [16], which is the initiator of Type II reactions found to be the dominant pathway in photosensitized degradations or transformations. In Type II mechanism the triplet state of the photosensitizers (^{3}MPc*) transfers energy to the ground state molecular oxygen ($^3O_2$) to give energetic singlet oxygen ($^1O_2$), Eq. (1), which in turn oxidizes the substrate (Subs), Eq. (2).

$$^3\text{MPc}* + {}^3O_2 \rightarrow {}^1O_2 \quad (1)$$

$$^1O_2 + \text{Subs} \rightarrow \text{Oxidationproducts} \quad (2)$$

In addition to their singlet oxygen generating abilities, open-shell metallo phthalocyanines (e.g. PdPc and PtPc) show high photostability [17,18] which is also an advantage over other metallophthalocyanines. This has made them prime candidates for photosensitization reactions. PdPc and PtPc derivatives have been reported to photosensitize oxidation reactions of 4-nitrophenol (4-NP) under homogeneous conditions [19]. A PdPc complex containing long alkyl chains was found to give high quantum yields for the phototransformation of 4-NP, hence it is employed in this work for the phototransformation of chlorophenols under homogeneous and heterogeneous conditions [20]. SWCNTs were chosen as support in heterogeneous catalysis because of ease of immobilization of MPcs due to the strong π–π interaction between SWCNTs and MPc complexes.

Thus this work investigates the photosensitizing properties of (2,3,9,10,16,17,23,24-octakis(dodecylthiophthalocyaninato) palladium(II) (PdODPc, Fig. 1) for the phototransformation of 4-chlorophenol and pentachlorophenol under homogeneous and heterogeneous conditions. For the latter, the PdPc complex was adsorbed on single walled carbon nanotubes (SWCNT).

* Corresponding author. Tel.: +27 46 603 8260; fax: +27 46 622 5109.
E-mail address: t.nyokong@ru.ac.za (T. Nyokong).

1381-1169/$ – see front matter © 2011 Elsevier B.V. All rights reserved.
doi:10.1016/j.molcata.2011.09.003

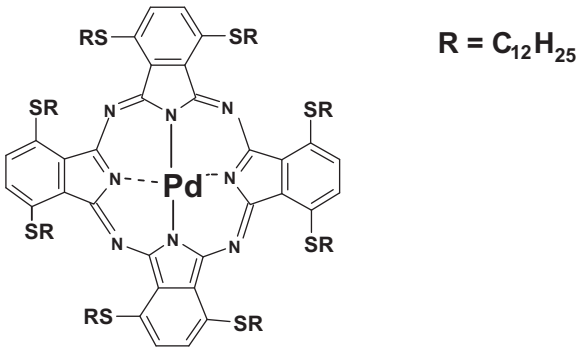

Fig. 1. Molecular structure of the photosensitizer (PdODPc) employed in this work.

2. Experimental

2.1. Materials

4-Chlorophenol (4-CP), pentachlorophenol (PCP), 2,3,5,6-tetrachloro-1,4-benzoquinone and hydroquinone were purchased from SAARCHEM. Dichloromethane (DCM) (SAARCHEM) was distilled before use. Distilled deionized water was used to prepare basic aqueous solutions of chlorophenols. Single walled carbon nanotubes (SWCNT, 0.7–1.2 nm in diameter and 2–20 μm in length) obtained from Aldrich were purified as reported in the literature [21], and briefly described in Section 2.2. Diethylamine and NaOH were used to increase the pH of organic and aqueous media respectively. Anthracene-9,10-bis-methylmalonate (ADMA) was from Sigma–Aldrich. The synthesis of the photocatalyst: 2,3,9,10,16,17,23,24-octakis (dodecylthio-phthalocyaninato) palladium(II) (PdODPc, Fig. 1) has been reported before [22].

2.2. Purification and functionalization of SWCNTs

SWCNTs were purified (oxidized) to form SWCNT–COOH by adding the raw SWCNTs (100 mg) to a mixture of HNO_3 and H_2SO_4 (3:1) [21] The resulting suspension was stirred at a temperature of 70 °C for 2 h. The final mixture was cooled to room temperature and washed with excess millipore water until a pH of 5 was obtained. The purified SWCNTs (SWCNT–COOH) were dried in an oven for 12 h.

2.3. Immobilization of PdODPc on SWCNT–COOH

The PdODPc (Fig. 1) complex was dissolved in DCM to give an absorbance of approximately 1 and 50 mg SWCNT–COOH was added and the mixture was stirred until there was no change in absorbance of the MPc. The mixture was centrifuged and the supernatant decanted, leaving the particles of SWCNT–COOH and the PdODPc adsorbed on their surface (represented as ads-PdODPc–SWCNT–COOH). The particles were washed with distilled deionized water, methanol and acetone and then air-dried for 24 h. The concentration of adsorbed MPcs was calculated from the differences in absorbances to be 1.0×10^{-8} M.

2.4. Equipment

X-ray powder diffraction patterns were recorded on a Bruker D8, Discover equipped with a proportional counter, using Cu-Kα radiation (λ = 1.5405 Å, nickel filter). Data were collected in the range from $2\theta = 5^\circ$ to 60°, scanning at 1° min^{-1} with a filter time-constant of 2.5 s per step and a slit width of 6.0 mm. Samples were placed on a silicon wafer slide. The X-ray diffraction data were treated using Eva (evaluation curve fitting) software. Baseline correction was performed on each diffraction pattern by subtracting a spline fitted to the curved background and the full-width at half-maximum values used in this study were obtained from the fitted curves.

Bruker Vertex 70-Ram II Raman spectrometer (equipped with a 1064 nm Nd:YAG laser and a liquid nitrogen cooled germanium detector) was used to collect Raman data. The Raman spectral data for the SWCNT–COOH, PdODPc, ads-PdODPc–SWCNT–COOH were obtained from their powdered samples.

2.5. Photochemical methods

Irradiation experiments were carried out with a tungsten lamp (100 W, 30 V) perpendicular to the direction of measurement. A 600 nm glass cut off filter (Schott) and a water filter were used to filter off ultraviolet and infrared radiations, respectively. An interference filter (Intor, 670 nm with a band width of 40 nm) was additionally placed in the light path before the sample, to ensure the excitation of the Q band only.

The intensity of the light reaching the reaction vessel was measured with a power meter (POWER MAX 5100, Molectron Detector Inc.) and was found to be 1×10^{15} photons cm^{-2} s^{-1}. The degradations of the analytes were monitored through their absorption peaks after each photolysis cycle on a Shimadzu UV-2550 UV–Vis spectrophotometer. A 1 cm pathlength UV–Vis spectrophotometric cell, fitted with a tight fitting stopper was used as the reaction vessel. For homogeneous reactions, experiments were carried out in DCM in which both the MPc and chlorophenols dissolved, while for heterogeneous reactions, experiments were carried out in aqueous media, using a suspension of PdODPc adsorbed on SWCNT–COOH. The photocatalysis products were analyzed using an Agilent Technologies 6820 GC system (HP 5973, using a HP-1 column). The participation of $^1O_2$ in the photolysis was confirmed by the addition of sodium azide, (a singlet oxygen quencher) to the photolysis reaction media. Singlet oxygen involvement was further confirmed by bubbling argon into the reaction media.

2.6. Photocatalysis parameters

2.6.1. Homogeneous reactions

The quantum yields of phototransformation of chlorophenols (Φ_{CP}) was calculated using Eq. (3) [23].

$$\Phi_{CP} = \frac{[C_0 - C_t]V}{I_{abs}t} \quad (3)$$

where C_0 and C_t are the concentrations of chlorophenols before and after irradiation respectively; V is the volume of the sample in the cell; t is the irradiation time. I_{abs} is given by Eq. (4)

$$I_{abs} = \frac{\alpha A I}{N_A} \quad (4)$$

where $\alpha = 1 - 10^{-A(\lambda)}$ ($A(\lambda)$ is the absorbance of the sensitizer at the irradiation wavelength), A is the irradiated area (3.14 cm^2), I is the intensity of light (1×10^{15} photons cm^{-2} s^{-1}) and N_A is Avogadro's constant.

Assuming the transformation of chlorophenols follows Type II reaction pathway, the three processes involved in the phototransformation of chlorophenols are represented by Eqs. (5)–(7).

$$^1O_2 \xrightarrow{k_d} {}^3O_2 \quad (5)$$

$$CP + {}^1O_2 \xrightarrow{k_q} {}^3O_2 \quad (6)$$

$$CP + {}^1O_2 \xrightarrow{k_a} \text{Products} \quad (7)$$

The rate constants involved are for the decay of $^1O_2$ (k_d, Eq. (5)), physical quenching of $^1O_2$ by the substrate (k_q, Eq. (6)) and the formation of oxidation products (k_a, Eq. (7)). Using Eqs. (5)–(7), the

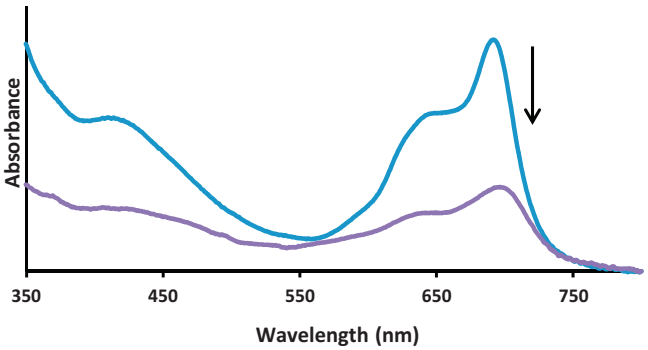

Fig. 2. Spectral changes showing the disappearance of PdODPc complex during its immobilization on SWCNT–COOH (200 mg), (initial concentration of **1a** = 1.2×10^{-5} mol dm^{-3}, time = 50 min); solvent DCM (basic media).

rate constants for the photodegradation of CP (CP = PCP or 4-CP) may be calculated using Eq. (8) [24].

$$\frac{1}{\Phi_{CP}} = \frac{1}{\Phi_{\Delta}}\left(\frac{k_q + k_a}{k_a} + \frac{k_d}{k_a[CP]}\right) \quad (8)$$

where Φ_{Δ} is the singlet oxygen quantum yield of the photocatalyst in DCM, the singlet oxygen decay rate constant, k_d, in DCM is 1.6×10^4 s^{-1} [25]. The rate constants: k_q and k_a can be determined by plotting of $1/\Phi_{CP}$ vs. 1/[CP] using Eq. (8).

Singlet oxygen quantum yield for ads-PdODPc–SWCNT–COOH was determined using ADMA as a singlet oxygen quencher in aqueous media. The quantum yields of ADMA (Φ_{ADMA}) for each irradiation cycle were calculated using Eq. (3) replacing Φ_{CP} with Φ_{ADMA} and the determined extinction coefficient of ADMA in aqueous media (ε = 9780 M L^{-1} cm^{-1} at 379 nm).

The singlet oxygen quantum yield (Φ_{Δ}) may then be calculated using Eq. (9) [23].

$$\frac{1}{\Phi_{ADMA}} = \frac{1}{\Phi_{\Delta}} + \frac{1}{\Phi_{\Delta}} \cdot \frac{k_d}{k_a} \cdot \frac{1}{[ADMA]} \quad (9)$$

where k_d is the decay constant of singlet oxygen and k_a is the rate constant for the reaction of ADMA with O_2 ($^1\Delta_g$). The value of Φ_{Δ} for the PdODPc was obtained as the intercept from the plot of $1/\Phi_{ADMA}$ vs. 1/[ADMA].

2.6.2. Heterogeneous reactions

For heterogeneous reactions, the Langmuir–Hinshelwood (L–H) (Eq. (10)) has been used to describe the competitive adsorption of substrates, reaction intermediates and phenolic oxidant products [26,27].

$$\frac{1}{\text{rate}} = \frac{1}{k_r} + \frac{1}{k_r K_{ads} C_0} \quad (10)$$

where k_r is the rate constant for the adsorption of CP, C_0 is the initial concentration of the substrate. K_{ads} is the adsorption coefficient and represents the equilibrium between the rates of adsorption and desorption [28].

3. Results and discussion

3.1. UV–Vis spectral studies for the formation of ads-PdODPc–SWCNT–COOH

The spectra of the PdODPc show extensive aggregation in DCM as has been reported before [22] (Fig. 2). Aggregation is judged by the presence of a broad band near 630 nm due to the aggregate, a sharper peak at 688 nm is due to the monomer.

On addition of SWCNT–COOH to solution of the PdODPc complex, followed by stirring, there was a decrease in absorbance as the latter adsorbed onto the former (Fig. 2). The resulting conjugate is represented as ads-PdODPc–SWCNT–COOH. SWCNTs are known to directly adsorb phenols such as 4-CP and PCP under investigation in this work [26,27]. In order to check if following immobilization of PdODPc complex onto SWCNT–COOH, there were still parts of SWCNT–COOH which were exposed, experiments were carried out where ads-PdODPc–SWCNT–COOH was immersed in a solution of 4-CP without photolysis. There was a slight decrease in the absorbance of 4-CP (~6%), showing that there were some empty sites on SWCNT–COOH where 4-CP adsorbed. The same background experiment was performed for PCP and similar results were obtained. The final spectrum following the adsorption of CP (4-CP or PCP) was used as the starting spectrum for all calculation done in this work. Experiments were also performed where PdODPc complex was suspended in a solution of 4-CP without photolysis, and there was no change in spectra, confirming that the latter does not react with the former in the absence of light. Experiments were also performed where SWCNT–COOH after adsorption of the CPs was photolysed without the sensitizer. There were no changes in absorbance which could be attributed to leaching of 4-CP (or its oxidation products) from the SWCNT–COOH. The same results were observed for PCP.

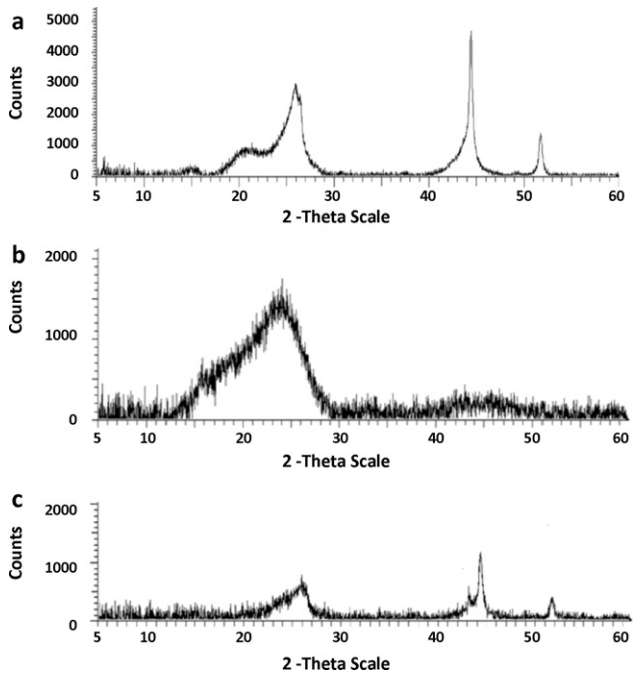

Fig. 3. XRD spectra of (a) SWCNT–COOH, (b) PdODPc complex and (c) ads-PdODPc–SWCNT–COOH.

3.2. Characterization ads-MPc–SWCNT–COOH

3.2.1. XRD

X-ray diffraction technique was used to confirm the formation of PdODPc–SWCNT–COOH composites. Fig. 3 shows the XRD spectra of SWCNT–COOH, PdODPc alone and ads-PdODPc–SWCNT–COOH. Fig. 3a (for SWCNT–COOH) shows sharp (2θ = 44.0° and 52.0°) and relatively broad (2θ = 21.0° and 26.1°) peaks that are indicative of the crystalline and amorphous natures of the SWCNT–COOH, respectively. Using international centre for diffraction data (ICDD) database, the peak at 2θ = 26.1° can be ascribed to (0 0 2) d-spacing of the SWCNT–COOH [29,30], while peaks at 2θ = 44.0° and 52.0° are characteristic of (1 0 0) [29], and (2 0 0) [30] reflections of carbon of the SWCNT–COOH, respectively. The only prominent peak in the XRD spectrum of PdODPc was a broad one at 2θ = 24.0° (Fig. 3b).

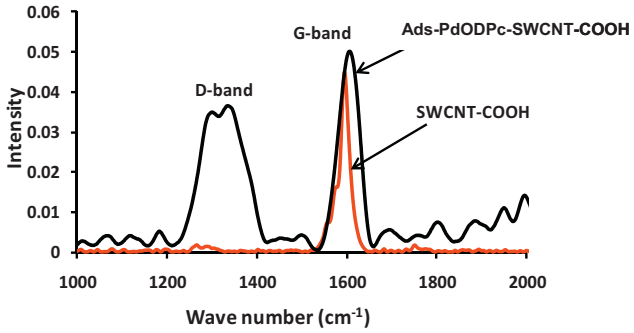

Fig. 4. Raman spectra of functionalized single walled carbon nanotube (SWCNT–COOH) and ads-PdODPc–SWCNT–COOH.

This peak is close to the (0 0 2) reflection of carbon and its broadness is an indication of the amorphousness of the complex. In the XRD of spectrum ads-PdODPc–SWCNT–COOH (Fig. 3c), the peak at 26.0° encompasses both PdODPc and SWCNT–COOH. It has been reported that the XRD peaks of carbon nanotubes become weak or disappear in the presence of phthalocyanines as a result of the amorphous state of the latter [31,32]. Thus the observed broadening of the SWCNT XRD peaks in the $2\theta = 20–30°$ region is due to the amorphous PdODPc on the SWCNT. The differences in spectra indirectly confirm the presence of a conjugate of SWCNT–COOH and PdODPc.

3.2.2. Raman spectroscopy

Raman spectroscopy is usually used for the characterization of disordered polycrystalline graphitic carbons. Raman spectroscopy is a fast, convenient and non-destructive analytical technique and can be used to some extent to quantify changes in the SWCNT–COOH using the ratio of D/G bands under fixed laser power intensity

Adsorption of MPc complexes may not cause extensive disruption to the carbon lattice due to the non-invasive π–π interactions i.e. preservation of the carbon nanotube structure, however small changes in the D/G ratio may indicate the presence of MPc on the SWCNT–COOH skeleton.

The G band for SWCNT–COOH shifted by 16 cm^{-1} for ads-PdODPc–SWCNT–COOH (Fig. 4). Functionalization of SWCNTs is known to enhance the D band [33–35]. There was an increase in D-band intensity compared to the G-band in the form of a D:G ratio (sp^3:sp^2 carbon ratio), with a ratio of 0.023 for SWCNT–COOH which increased to 0.72 for ads-PdODPc–SWCNT–COOH, this confirms functionalization of SWCNT–COOH with PdODPc complex.

3.2.3. Singlet oxygen generation capacity of ads-MPc–SWCNT–COOH

Since singlet oxygen is thought to be involved in the photocatalysis mechanism, its generation by ads-PdODPc–SWCNT–COOH was investigated. Interference filter was employed to ensure the excitation of the high energy peak due to the monomer of the adsorbed Pc on ads-PdODPc–SWCNT–COOH. An aqueous solution of 6.0×10^{-5} mol dm^{-3} ADMA containing the ads-PdODPc–SWCNT–COOH was successively irradiated at the Q-band PdODPc, centrifuged and decanted into UV–Vis cell and the absorbance recorded. The absorbance of ADMA at 379 nm showed a linear decrease, confirming that singlet oxygen is formed by ads-PdODPc–SWCNT–COOH in the presence of ADMA. The spectrum of the PdODPc was not observed since the complex acted as heterogeneous catalyst in the reaction. Singlet oxygen values were determined using Eq. (9), and the Φ_Δ value (=0.27) of ads-PdODPc–SWCNT–COOH was obtained.

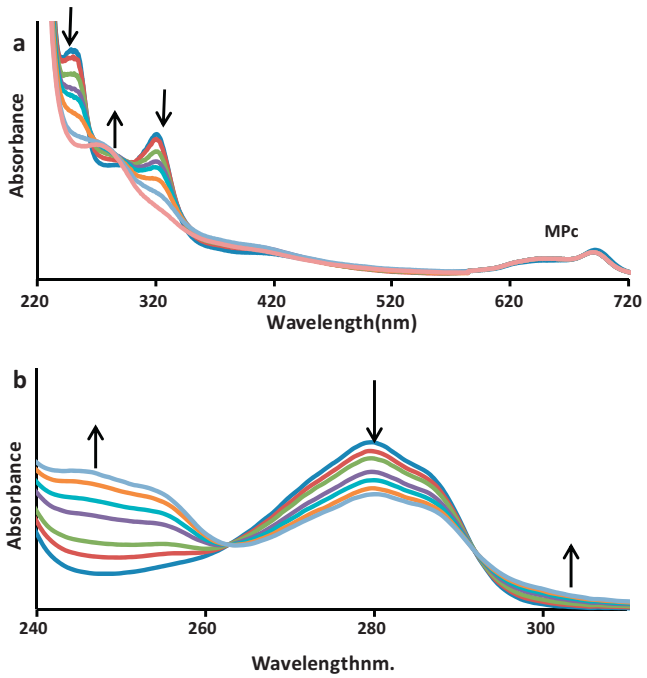

Fig. 5. Spectral changes showing the disappearance of (a) PCP and (b) 4-CP during homogeneous photolysis in the presence of PdODPc (300 mg L−1) in DCM.

3.3. Homogeneous catalysis of 4-CP and PCP

3.3.1. Spectroscopic characterization

Fig. 5a shows the spectral changes observed for pentachlorophenol (PCP) during homogeneous photolysis in the presence of the photosensitizer (PdODPc) conducted in DCM. These studies were carried out in aqueous solution at pH 9 because phenolate ions which are more oxidizable are predominant at high pH. There was a decrease in the concentration of PCP during irradiation (with time) in the presence of PdODPc complex while the concentration of the complex remained unchanged due to its high photostability as indicated by the relative lack of change in the absorbance of the Q-band of the complex at around 688 nm. The peaks due to PCP observed at 252 nm and 322 nm started disappearing with simultaneous appearance of a peak around 273 nm due to the formation of the product(s). The same trend was observed for 4-chlorophenol in the presence of photosensitizer with reduction in the absorbance of the peak at 280 nm (Fig. 5b). The Φ_{CP} was calculated from the initial rate of disappearance of the CP using Eq. (3). Effects of the PdODPc absorption in the B band region were corrected by subtraction of its absorption from for all calculations.

Because the concentration of the catalyst might have an effect on the phototransformation of the analytes, experiments were conducted using various concentrations of the catalysts ranging from 50 mg L^{-1} and 600 mg L^{-1} and the initial rate of disappearance of CP determined and Φ_{CP} were calculated.

As shown in Fig. 6, as the concentration of the sensitizer increased, the Φ_{CP} values increased until a maximum was reached around which the plot flattened and then there was a decline. The flattening could be due to inability of additional catalyst to bring commensurate increase in quantum yield as aggregation began to set in. The decrease in Φ_{CP} with increase in PdODPc concentration could be due to extensive aggregation of the molecules at high concentrations. The optimum concentrations of the sensitizer were 350 mg L^{-1} for 4-CP and 300 mg L^{-1} for PCP. The percentage conversion of 4-CP was 91% and for PCP, the values was 70% (Table 1).

Table 1
Photocatalytic parameters for phototransformation of 4-CP and PCP in basic media.

Substrate	Optimum catalyst conc. (mg L^{-1})	Φ_{CP}	$k_a = k_d/\Phi_\Delta$ Slope(mol^{-1} L s^{-1})	$k_q + k_a$ (mol^{-1} L s^{-1})	% conversion (24 h reaction time)
4-CP	350	9×10^{-4}	3.4×10^4	5.2×10^4	91
PCP	300	2×10^{-5}	5.6×10^2	8.2×10^4	70

3.3.2. Kinetics of photocatalysis

The rate constant for homogeneous photo-oxidation, k_a, was estimated from the slope of the linear plot of $1/\Phi_{CP}$ vs. 1/[CP] (Eq. (8)). k_a equals k_d/Φ_Δ Slope where k_d is the singlet oxygen decay constant in DCM (1.6×10^4 [25]), and Φ_Δ is the singlet oxygen quantum yield of the sensitizer in DCM ($\Phi_\Delta = 0.26$) [19].

Using k_a values as an indication of photodegradation efficiency, Table 1 shows that photooxidation of 4-CP occurred faster than for PCP, due to plurality of the electron withdrawing chloride substituents which will make the ring difficult to oxidize for the latter. The breakdown of the aromatic ring has been reported to be slightly faster for 4-CP compared to PCP using semi-conductor particles [36].

The quenching effects of the CPs on the singlet oxygen was estimated from ($k_q + k_a$) calculated from the intercept $1/\Phi_{CP}$ vs. 1/[CP] (Eq. (8)). Comparison of the ($k_q + k_a$) with k_a or estimation of k_q from the two gives the deactivation or quenching of singlet oxygen via other routes apart from oxidation reaction with chlorophenols. The values of ($k_q + k_a$) for the sensitizer employed in this work were 8.2×10^4 and 5.2×10^4 mol^{-1} dm^3 s^{-1} for PCP and 4-CP respectively while k_a values were 5.6×10^2 and 3.4×10^4 mol^{-1} dm^3 s^{-1} for PCP and 4-CP, respectively (Table 1). The implication of larger ($k_q + k_a$) compared to k_a for PCP is that considerable amount of physical (chemically unproductive) quenching of singlet oxygen via Eq. (6) took place during the reactions for PCP, hence the lower rate constant for PCP compared to 4-CP.

3.4. Heterogeneous reactions

For heterogeneous reactions, PdODPc is adsorbed onto the SWCNT–COOH. On visible light irradiation, PdODPc is excited to the triplet state, generating reactive oxygen species such as singlet oxygen. It is the reactive oxygen species which are involved in catalysis. For heterogeneous photosensitization, the optimum catalyst (as ads-PdODPc–SWCNT–COOH) loading was determined using 1.00×10^{-4} M solution of 4-CP or PCP, while varying the catalyst concentration from 100 mg L^{-1} to 800 mg L^{-1}. The decrease in absorption spectra of the PdODPc complex as it adsorbs onto SWCNT–COOH was recorded for each catalyst concentration as shown by Fig. 2. Then the ads-PdODPc–SWCNT–COOH for each catalyst concentration was employed for the phototransformation of CPs. The initial rate of reaction for each catalyst concentration was determined. The removal of the CPs increased linearly with catalyst concentration until it reached 500 mg L^{-1} for both PCP and 4-CP (figure not shown), after which a decrease was observed probably due to shielding effect of the excess catalyst causing reduction in the penetration of light. The percentage conversion of 4-CP was 42% and for PCP, the value was 30%, Table 2 (at the optimum catalyst concentration), hence the values are lower than for homogeneous catalysis. No leaching of the PdODPc from the SWCNT–COOH is expected since the latter is insoluble in water.

The kinetics of heterogeneous transformation of both 4-CP and PCP fitted into pseudo first-order reaction kinetics which may be expressed as $\ln(C_0/C_t) = k_{obs}t$. The apparent rate constant (k_{obs}) was obtained from the slopes in Fig. 7 (for PCP) for the two substrates at different concentrations ranging from 4×10^{-5} to 1.0×10^{-4} M. The apparent rate of reaction k_{obs} for ads-PdODPc–SWCNT–COOH, Table 2, shows that the more dilute the CP solutions, the higher the apparent rate of transformation. The k_{obs} values ranged between 1.21×10^{-3} min^{-1} and 3.12×10^{-3} min^{-1} for 4-CP and 1.80×10^{-3} min^{-1} and 4.00×10^{-3} min^{-1} for PCP for concentrations of 4, 6, 8 and 10×10^{-5} M. Thus the values are slightly higher for PCP.

It is important to establish if the transformation reaction takes place in the adsorbed state and to determine the adsorption coefficient. Langmuir–Hinshelwood model (Eq. (10)) was employed for these studies.The plots of reciprocal of initial rate of phototransformation vs. reciprocal of initial concentration of CPs (Fig. 8) give k_r as the intercept, and the adsorption coefficient (K_{ads}) was determined from slope. The plots were found to be linear with a non-zero intercept for both 4-CP and PCP. The values of k_r and K_{ads} are listed in Table 2. According to Table 2, adsorption rate (k_r) was lower for 4-CP with a value of 6.06×10^{-7} M min^{-1} compared to PCP 1.02×10^{-6} M min^{-1}. The values of adsorption coefficient ($K_{ads} \gg 1$) suggest that adsorption was more favored over desorption for both substrates with adsorption of 4-CP being the more favored because of its higher K_{ads} values.

3.5. Catalyst stability

Following use in the transformation of chlorophenols, the ads-PdODPc–SWCNT–COOH were cleaned by rinsing in water, dried and reused for the phototransformation. Fig. 9 shows the plots

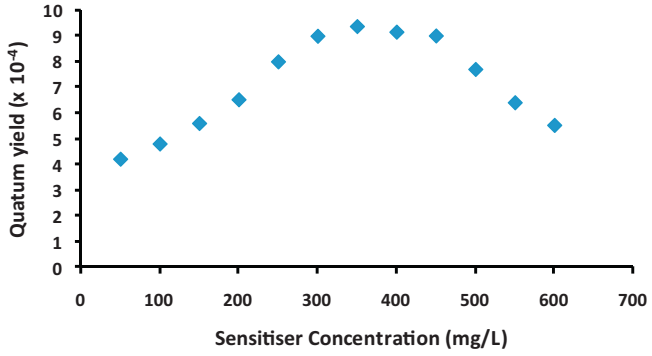

Fig. 6. Plot of $\Phi_{4\text{-CP}}$ vs. concentration of photosensitizer to determine the optimum sensitizer concentration for phototransformation of 4-CP (concentration = 1.00×10^{-4} M) in DCM.

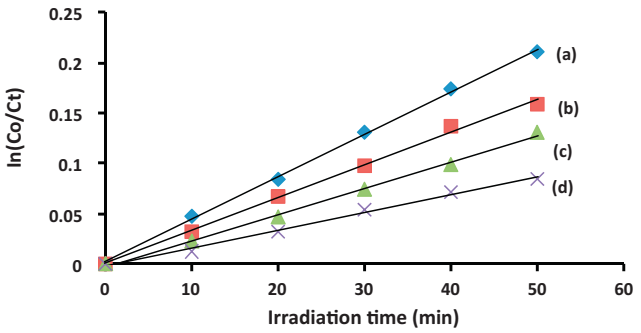

Fig. 7. Kinetic plot for ads-PdODPc–SWCNT–COOH in photooxidation of PCP. Starting concentrations are (a) 4×10^{-5} M, (b) 6×10^{-5} M, (c) 8×10^{-5} M and (d) 10×10^{-5} M in water.

Table 2
Langmuir–Hinshelwood (L–H) parameters for the phototransformation of 4-CP and PCP on ads-PdODPc–SWCNT–COOH in basic media.

Substrate	Conc. (M)	k_{obs} (min^{-1}) (10^{-3})	k_r ($M\,min^{-1}$)	K_{ads} (M^{-1})	%conversion (24 h reaction time)
4-CP	4.00×10^{-5}	3.12	6.06×10^{-7}	2.7×10^{3}	42
	6.00×10^{-5}	2.27			
	8.00×10^{-5}	1.92			
	1.00×10^{-4}	1.21			
PCP	4.00×10^{-5}	4.00	1.02×10^{-6}	5.56×10^{2}	30
	6.00×10^{-5}	3.30			
	8.00×10^{-5}	2.60			
	1.00×10^{-4}	1.80			

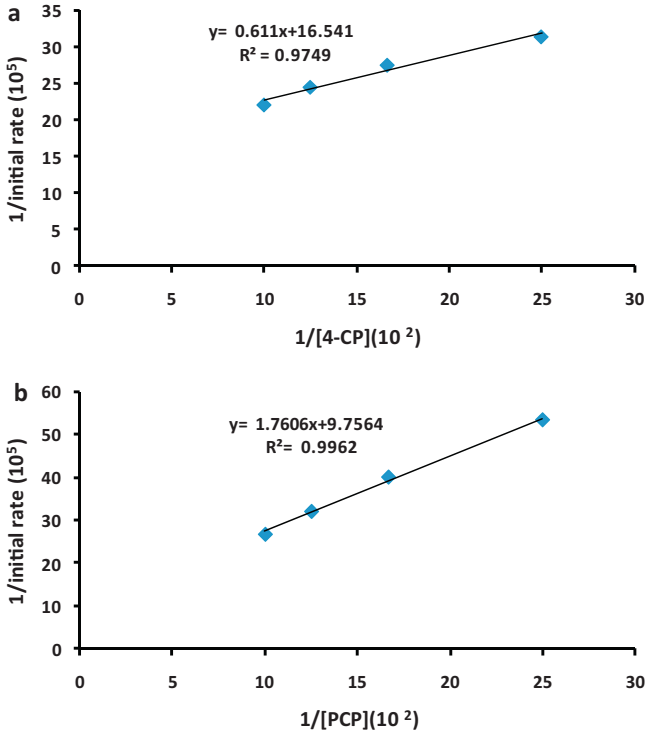

Fig. 8. Plots of reciprocals of initial rate of phototransformation vs. initial concentration of CP (a) 4-CP and (b) PCP using ads-PdODPc–SWCNT–COOH.

of concentration vs. time, for the first, second and third uses of ads-PdODPc–SWCNT–COOH for the phototransformation of fresh solution of PCP. The rate changes remained approximately the same between $7.85 \times 10^{-7}\,M\,min^{-1}$ and $7.82 \times 10^{-7}\,M\,min^{-1}$ from the first to the third use in the case of 4-CP (figure not shown). But for PCP, Fig. 9, the story was completely different as the rate

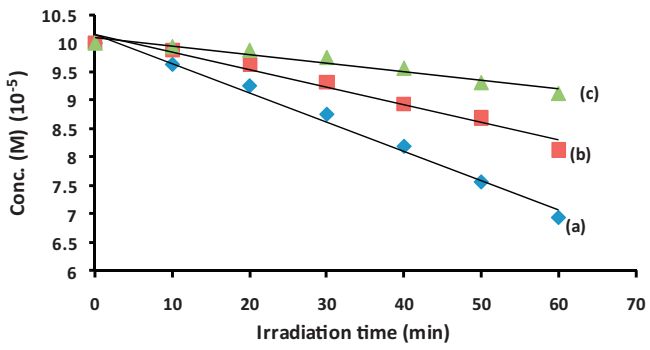

Fig. 9. Plots of concentration vs. time for the reuse of ads-PdODPc–SWCNT–COOH for the phototransformation of PCP. (a) 1st use, (b) 2nd (re-use) and (c) 3rd (re-use) in water.

dropped drastically from $5.00 \times 10^{-7}\,M\,min^{-1}$ for the first use to $3.00 \times 10^{-7}\,M\,min^{-1}$ for the second use and $1.00 \times 10^{-7}\,M\,min^{-1}$ for the third use. The drastic reduction might be due to permanent adsorption of intermediates or products on the surface of the catalyst thereby reducing its adsorption activities. It is now well established that the upon oxidation, chlorophenols form polymers which have diffusion limitation from the catalyst, blocking the surface [37,38]. Hence the observed decrease in activity of ads-PdODPc–SWCNT–COOH following use is not surprising. The differences in the degree of deactivation of the surfaces by phenolic compounds and their oxidation products, have been explained in terms of the different structure (hence permeability) of the polymeric formed, where the more regular and dense polymer structures deactivate the surface more rapidly [39]. Thus the observed deactivation of ads-PdODPc–SWCNT–COOH by PCP implies that the products from by the oxidation of PCP form a dense polymer on the surface of the ads-PdODPc–SWCNT–COOH particles.

This was confirmed by repeating the kinetic of the reactions for the reuse (second use) in the transformation of each of the substrate. While the adsorption coefficient (K_{ads}) and the adsorption rate (k_r) remained the same for 4-CP, they both drastically decreased in the case of PCP from $1.02 \times 10^{-5}\,M\,min^{-1}$ and $556\,M^{-1}$ to $5 \times 10^{-6}\,M\,min^{-1}$ and $132\,M^{-1}$ for k_r and K_{ads}, respectively, implying that in the case of PCP the number of binding sites are reduced significantly after use. When not in use the ads-PdODPc–SWCNT–COOH conjugates showed long-term stability (of months when stored in the dark) in that they gave the same initial rates when used for chlorophenol degradation.

3.6. Photodegradation products and mechanism

GC was used to determine the products of homogeneous and heterogeneous phototransformation processes for the two substrate by comparing the retention times of standards of likely products such as fumaric acid, 1,4-benzoquinone, hydroquinone and tetrachlorobenzoquinone. Two peaks due to the products were observed in the gas chromatogram traces for homogeneous photosensitization of 4-CP. These are: hydroquinone at 5.54 min which appeared in minute quantity (~5% of products) and 1,4-benzoquinone (Scheme 1), the major product which appeared at 3.00 min, under homogeneous catalysis. These peaks were all confirmed during GC analysis by spiking with the respective standards. During heterogeneous catalysis (of 4-CP) the GC traces showed that the same products were formed but with higher proportion of hydroquinone (~20% of products). It is also important to mention that when oxygen was bubbled for longer period of time the proportion of hydroquinone in the products decreased while that of benzoquinone increased suggesting that singlet oxygen might be directly responsible for the production of benzoquinone while hydroquinone might be produced through Type I pathway (but in small amounts). This was also confirmed by bubbling argon through a reaction medium before photolysis. The reaction gave

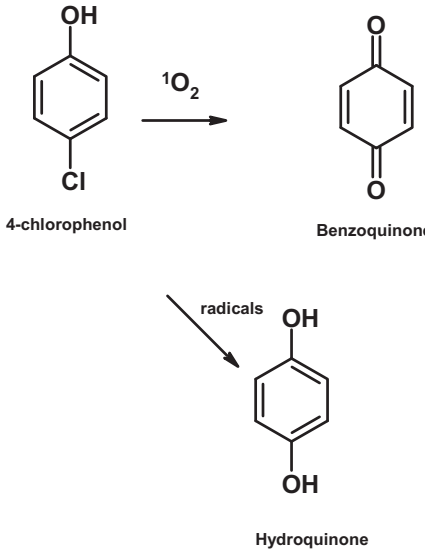

Scheme 1. Proposed mechanism for the phototransformation of 4-CP on ads-PdODPc–SWCNT–COOH.

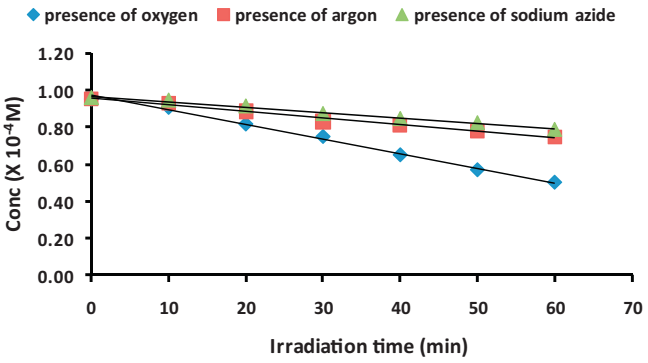

Fig. 10. Demonstration of the effect of sodium azide and argon on 4-CP phototransformation rate using ads-PdODPc–SWCNT–COOH.

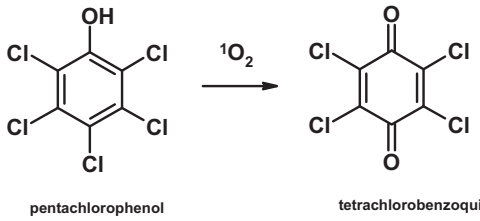

Scheme 2. Proposed mechanism for the phototransformation of PCP on ads-PdODPc–SWCNT–COOH.

a higher proportion of hydroquinone (70% of products) though rate of reaction (4.00×10^{-7} M min^{-1}) was slower than when oxygen was bubbled (8.00×10^{-7} M min^{-1}) (Fig. 10). Photolysis was also performed in the presence of a singlet oxygen scavenger, NaN_3, the reaction rate was similar to when argon was bubbled with a rate of 3.00×10^{-7} M min^{-1}. Both homogeneous and heterogeneous photosensitization for pentachlorophenol gave 2,3,5,6-tetrachloro-1,4-benzoquinone (Scheme 2) with homogeneous reaction giving 70% conversion as compared with 30% for heterogeneous reaction. Introduction of singlet oxygen scavenger halted the reaction suggesting that the only pathway available for this transformation is the Type II pathway.

4. Conclusions

This work showed that PdODPc is capable of both homogeneous and heterogeneous photo-oxidation of 4-chlorophenol and pentachlorophenol. The oxidation of both substrates was faster under homogeneous conditions and gave higher percentage conversion than for heterogeneous catalysis. It was confirmed that singlet oxygen played a role in the phototransformation of both substrates. Direct oxidation of 4-chlorophenol appeared to result in the formation of benzoquinone while hydroquinone seemed to be the product from Type I reaction pathway.

Acknowledgements

This work was supported by the Department of Science and Technology (DST) and National Research Foundation (NRF) of South Africa through DST/NRF South African Research Chairs Initiative for Professor of Medicinal Chemistry and Nanotechnology and Rhodes University. T.O. thanks African Laser centre for graduate bursary.

References

[1] A. Mylonas, E. Papaconstantinou, J. Photochem. Photobiol. A Chem. 94 (1996) 77–82.
[2] H. Roques, Chemical Water Treatment, VCH Verlag, Weinheim, Germany, 1996.
[3] A. Mylonas, E. Papaconstantinou, Polyhedron 15 (1996) 3211–3217.
[4] A. Sorokin, B. Meunier, Chem. Eur. J. 2 (1996) 1308–1317.
[5] A. Sorokin, J.-L. Seïris, B. Meunier, Science 268 (1995) 1163–1165.
[6] A. Sorokin, L. Fraisse, A. Rabion, B. Meunier, J. Mol. Catal. A 117 (1997) 103–114.
[7] S. Rismayani, M. Fukushima, A. Sawada, H. Ichikawa, K. Tatsumi, J. Mol. Catal. A Chem. 217 (2004) 13–19.
[8] M. Fukushima, K. Tatsumi, Biores. Tech. 97 (2006) 1605–1611.
[9] M. Fukushima, K. Tatsumi, Toxicol. Environ. Chem. 85 (2003) 39–49.
[10] M. Fukushima, K. Tatsumi, Environ. Sci. Technol. 35 (2001) 1771–1778.
[11] N. Nensala, T. Nyokong, J. Mol. Catal. A 164 (2000) 69–76.
[12] E. Chamarro, A. Marco, S. Esplugas, Water. Res. 35 (2001) 1047–1051.
[13] B. Meunier, A. Sorokin, Acc. Chem. Res. 30 (1997) 470–476.
[14] M. Alvaro, E. Carbonell, M. Esplá, H. Garcia, Appl. Catal. B Environ. 57 (2005) 37–42.
[15] V. Iliev, V. Alexiev, L. Bilyarska, J. Mol. Catal. A Chem. 137 (1999) 15–26.
[16] T.B. Ogunbayo, T. Nyokong, J. Mol. Struc. 973 (2010) 96–103.
[17] A. Sun, Z. Xiong, Y. Xu, J. Hazard. Mater. 152 (2008) 191–195.
[18] X. Xue, Y. Xu, J. Mol. Catal. A Chem. 276 (2007) 80–85.
[19] T.B. Ogunbayo, E. Antunes, T. Nyokong, J. Mol. Catal. A Chem. 334 (2011) 123–129.
[20] T.B. Ogunbayo, T. Nyokong, J. Mol. Catal. A Chem. 337 (2011) 68–76.
[21] J. Liu, A.G. Rinzler, H. Dai, J.H. Hafner, R.K. Bradley, P.J. Boul, A. Lu, T. Iverson, K. Shelimov, C.B. Huffman, F. Rodriguez-Macias, T.Y.-S. Shon, R. Lee, D.T. Colbert, R.E. Smalley, Science 280 (1998) 1253–1256.
[22] T.B. Ogunbayo, A. Ogunsipe, T. Nyokong, Dyes Pigm. 82 (2009) 422–426.
[23] W. Spiller, H. Kliesch, D. Worhle, S. Hackbarth, B. Roder, G. Schnurpfield, J. Porphyr. Phthalocyan. 2 (1998) 145–158.
[24] K. Ozoemena, N. Kuznetsova, T. Nyokong, J. Mol. Catal. A Chem. 176 (2001) 29–40.
[25] F. Wilkinson, J.G. Brummer, J. Phys. Chem. Ref. Data 10 (1981) 825.
[26] H. Al-Ekabi, N. Serpone, J. Phys. Chem. 92 (1988) 5726–5731.
[27] D.D. Dionysiou, A.P. Khodadoust, A.M. Kern, M.T. Suidan, I. Baudin, J.-M. Laîné, Appl. Catal. B Environ. 24 (2000) 139–155.
[28] K.J. Laider, J.H. Meiser, B.C. Sanctuary, Physical Chemistry, fourth ed., Houghton Mifflin Company, Boston, 2003, p. 933.
[29] M. Terrones, W.K. Hsu, A. Schwoerer, K. Prassides, H.W. Kroto, D.R. Walton, Appl. Phys. A 66 (1998) 307–317.
[30] Y. Zhang, X. Sun, L. Pan, H. Li, Z. Sun, C. Sun, B.K. Tay, J. Alloys Compd. 480 (2009) L17–L19.
[31] K. Wang, J.-J. Xu, K.-S. Tang, H.-Y. Chen, Talanta 67 (2005) 798–805.
[32] Z. Xu, H. Li, K.-Z. Li, Y. Kuang, Y. Wang, Q. Fu, Z. Cao, W. Li, Cryst. Growth Design 9 (2009) 4136–4141.
[33] B.K. Price, J.M. Tour, J. Am. Chem. Soc. 128 (2006) 12899–12904.
[34] J. Jiang, R. Saito, A. Grüneis, S.G. Chou, Ge.G. Samsonidze, A. Jorio, G. Dresselhaus, M.S. Dresselhaus, Phys. Rev. B 71 (2005), 045417/25.
[35] M.D. Ellison, P.J. Gasda, J. Phys. Chem. C 112 (2008) 738–740.
[36] M. Barbeni, E. Pramauro, E. Pelizzeti, Chemosphere 14 (1985) 195–208.
[37] Z. Ežerskis, Z. Jusys, Pure Appl. Chem. 73 (2001) 1929–1940.
[38] R. Li, P.E. Savage, D. Szmukler, AIChE J. 39 (1993) 178–187.
[39] Z. Ežerskis, Z. Jusys, J. Appl. Electrochem. 31 (2001) 1117–1124.